COUPLED DEM – CFD MODELLING OF THE IRONMAKING BLAST FURNACE

Allert ADEMA[1,2*], Yongxiang YANG[2] and Rob BOOM[1,2,3]

[1] Materials innovation institute, M2i, Delft, THE NETHERLANDS
[2] Department of Materials Science and Engineering, Delft University of Technology,
Mekelweg 2, 2628 CD, Delft, THE NETHERLANDS
[3] Corus Research Development & Technology, IJmuiden, THE NETHERLANDS
*Corresponding author, E-mail address: A.T.Adema@tudelft.nl

ABSTRACT

The modern ironmaking blast furnace is a complex counter-current multi-phase high temperature reactor; its highly interdependent parameters make process simulation a very challenging task. Any accurate process simulation requires a realistic model of the solid and gas flow as well as their interaction. This work presents a isothermal coupled simulation linking solid flow, modelled by the Discrete Element Model (DEM), to gas flow modelling by CFD. The use of the DEM method ensures a realistic solid flow based on particle properties and fully takes into account its discrete nature. The main focus of the project lies on the cohesive zone, where the ore fed into the blast furnace softens and melts. The ore layers, alternating with coke layers, become increasingly impermeable and generate increased friction to the solid burden flow. The cohesive zone is critical to blast furnace performance and stability due to its influence on the gas and solid flow. Coupling of the DEM and the CFD methods gives the possibility of introducing thermodynamics and reaction kinetics into the continuous phase. The combination of the modelling techniques allows for simulation of the blast furnace process including realistic solid burden flow.

NOMENCLATURE

m mass (kg)
V volume (m^3)
t time (s)
p pressure (Pa)
$\mathbf{F}$ force (N)
g gravitational constant (m/s^2)
E Young's modulus
R radius (m)
S stiffness (N/m)
e coefficient of restitution
I moment of inertia (kg/m^2)
T torque (Nm)
P momentum sink (N/m^3)
C_D drag coefficient
A surface area (m^2)
Re   Reynolds number

δ particle overlap (m)
ω angular velocity (s^{-1})
μ coefficient of friction
ρ density (kg/m^3)

INTRODUCTION

The modern ironmaking blast furnace is a complex counter-current multi-phase high temperature reactor, and the highly interdependent parameters make process simulation a very challenging task. This paper will present the outline of a proposed modelling approach which will contribute to a more accurate prediction of the properties of the blast furnace cohesive zone as well as the results of the solid flow model combined with a CFD gas flow model.

Blast Furnace Ironmaking

Figure 1 shows a cross section of the blast furnace as is used in ironmaking. The furnace is fed with two types of solids: the ferrous materials containing iron oxides and the coke containing carbon. Ore and coke are charged at the top in layers and as they descend through the furnace they are heated and the iron oxides, hematite (Fe_2O_3) and magnetite (Fe_3O_4), are reduced by CO and H_2 gas to wustite ($Fe_{0.95}O$). The reduction gas CO is generated by the reaction of hot oxygen-enriched air blown into the furnace through the tuyeres with the coke particles, H_2 by reduction of water in the feed and blast. This creates a void space in the blast furnace called the raceway, extending 1-2 m into the furnace, beyond which exists a volume of very slow moving coke particles known as the "deadman". The molten iron and the slag flow through the deadman and are tapped from the hearth.

The cohesive zone, where the ore fed into the blast furnace softens and melts, is critical to blast furnace performance and stability due to its influence on the gas and solid flow. When temperatures of approximately 1200˚C are reached, the ore layers start softening and melting causing the permeability to the ascending reduction gasses to decrease significantly, leaving only the coke slits open to gas flow as illustrated in Figure 1. This zone, containing the low permeability ore layers and the coke slits, is known as the cohesive zone. The formed molten slag and iron trickle down from the cohesive zone through the coke bed below and into the hearth. The solids consumption in the blast furnace which drives the solid flow is can only be attributed for 25% at the tuyeres due to coke gasification. The remainder is due to melting of the burden materials and coke consumption by hot metal carburisation and direct reduction. Both of these occur in and around the cohesive zone.
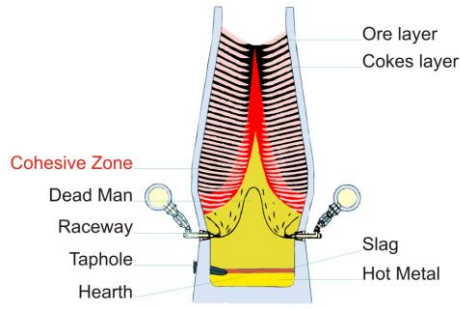
Figure 1: Zones in the Blast Furnace.

Project description

The aim of this project is the development of a realistic prediction model for the cohesive zone properties, including its shape, location, structure, permeability and mineralogical changes. This will be used to predict status changes of the cohesive zone due to changes of the operating conditions such as feed variations. The tool used to develop such a model is a combination of various modelling techniques. For the materials flow simulation a coupled DEM-CFD model is used. The DEM model can deliver accurate and fundamental solid flow modelling as is applied in previous work by Adema (2008). Here it is coupled with CFD for continuum modelling of the gas flow and can be further extended for liquid and/or fine particle phases. For both models commercial software is used: Fluent (www.fluent.com), a general purpose CFD package and EDEM (www.dem-solutions.com), a general purpose DEM package. The DEM-CFD coupling is made using EDEM's coupling module with Fluent. All simulations are iso-thermal. The model described here does not include cohesive forces between particles or particle softening. And thus at this stage it cannot realistically predict all the cohesive zone properties.

The cohesive zone properties are highly dependent on the softening, melting and chemical reactions; therefore, the DEM-CFD coupled model will be combined with a burden softening and melting model based on thermodynamic and kinetic models. The combination of the basic models for DEM and CFD into the coupled burden flow model forms the general framework of the final model. The combination of the thermodynamic and kinetic models provide the fundamentals of the ironmaking process: the metallurgical physical chemistry. Implementation of this into the flow model will result in the overall model.

Blast furnace modelling

In its long history a large amount of research has gone into the blast furnace in which modelling has played a significant part. Both continuum models and more recently discrete models have been developed.

Continuum approach

Using the continuum approach, the solid particles are represented by a continuous flow phase. The approach can give good results on a macroscopic level but is highly dependent on empirical relations, rather than fundamentals. As mentioned, a significant amount of research has been done, example of which is the four-fluid or multi-fluid model by Yagi (1993) in which solid flow is described by the viscous flow model and further applied by Austin et al. (1997), De Castro et al. (2002) and

Nogami et al. (2005). The hypo-plasticity model for solid flow was developed by Zaïmi et al. (2000, 2004). The great advantage of this model over the previous is the ability to predict the deadman instead of requiring a predefined one. A solid flow model was published by Zhang et al. (1998, 2002), where the stress due to flowing particle interaction is composed of two components; rate-dependent and rate-independent. Two examples from industry are the MOGADOR model by Danloy et al. (2001) and the BRIGHT model by Matsuzaki et al. (2006).

Discrete approach

In this approach the individual particles are modelled by tracking the motion of every particle as well as the collisions between particles and between particles and their environment (e.g. walls). The method allows for simulations based on individual particle interactions without requiring empirical constants. Examples of using the discrete approach can be found in the work of Zhou et al. (2008), who modelled solid flow in the blast furnace with and without gas flow. Both Kawai and Takahashi (2004) and Nouchi et al (2003, 2005) investigated the influence of storing and tapping liquid in the hearth on solid behaviour. The major disadvantage of the DEM method is the high computational requirements making it impossible to model large full scale industrial processes.

DEM MODELLING

In the Discrete Element Method every individual particle is tracked and its motion is calculated based on Newton's second law of motion and the governing equation for the translational motion can be written as:

$$m_i \frac{d\mathrm{v}_i}{dt} = \left(\mathrm{F}_n + \mathrm{F}_n^d \right) + m_i \mathrm{g} + \mathrm{F}_D \qquad (1)$$

where, particle i has mass m_i, and velocity $\mathbf{v}_i$. The right hand side contains terms for contact, gravity and drag forces. This general governing equation for the solid motion is solved with the general purpose DEM software package EDEM. In Equation (1), the collision forces are calculated using the Herz-Mindlin No Slip contact model based on the work of Mindlin and Deresiewicz (1953). The two forces governing the contact model are the normal force, F_n, and the normal damping force, F_n^d. The former is a function of the equivalent Young's modulus $E\textbf{*}$ (stress-strain relation) according to Equation (2) where $R\textbf{*}$ and δ_n are the equivalent radius and normal overlap. Damping force shown in Equation (3) is a function of the particle properties; equivalent mass $m\textbf{*}$ and the normal component of the relative velocity v_n^{rel}; and material properties; the normal stiffness S_n and the coefficient of restitution e.

$$\mathrm{F}_n = \frac{4}{3} E^* \sqrt{R^*} \delta_n^{3/2} \qquad (2)$$

$$\mathrm{F}_n^d = -2\sqrt{\frac{5}{6}} \beta \sqrt{S_n m^*} \mathrm{v}_n^{rel} \qquad (3)$$

with: $\beta = \dfrac{\ln e}{\sqrt{\ln^2 e + \pi^2}}$

and $S_n = 2E^* \sqrt{R^* \delta_n}$

Besides translational motion as governed by Equation (1) particles also undergo rotational motion, which is governed by Equation (4).

$$I_i \frac{d\omega_i}{dt} = \mathbf{T}_i + \mathbf{M}_i \qquad (4)$$

where I_i is the moment of inertia, ω_i the angular velocity, $\mathbf{T}_i$ the torque generated by the tangential forces and $\mathbf{M}_i$ is the torque generated by the rolling friction. The tangential force torque given in equation (5) depends on two components: the tangential force F_t and the tangential damping force F_t^d. The former is shown in Equation (6), where δ_t is the tangential overlap and S_t the tangential stiffness; and the latter in Equation (7) where v_t^{rel} is the relative tangential velocity.

$$\mathbf{T}_i = \mathbf{R}_i \times \left(\mathbf{F}_t + \mathbf{F}_t^d \right) \qquad (5)$$

$$\mathbf{F}_t = -S_t \delta_t \qquad (6)$$

with: $S_t = 8G^* \sqrt{R^* \delta_n}$

$$\mathbf{F}_t^d = -2\sqrt{\frac{5}{6}} \beta \sqrt{S_t m^*} \, v_t^{rel} \qquad (7)$$

Coulomb friction, $\mu_s F_n$ with μ_s the coefficient of static friction, limits the tangential force. Rolling friction is included in the equations by applying the negative torque shown in Equation (8), where μ_r is the coefficient of rolling friction, R_i the distance from the centre of mass to the contact point and ω_i the unit angular velocity vector at the contact point.

$$\mathbf{M}_i = -\mu_r F_n R_i \omega_i \qquad (8)$$

For an extensive background on the theory of discrete particle modelling we would like to refer to Zhu et al. (2007).DEM - CFD Coupling

The EDEM – Fluent Coupling Module is used to couple the DEM simulation with CFD, and uses the existing Eulerian – Eulerian multiphase model in Fluent. Equations (9) and (10) show the continuity and momentum equations for the gas phase; where ε is the volume fraction, ρ the density, $\mathbf{u}$ the velocity, μ the viscosity, p the pressure and S the momentum sink. The momentum equation is based on the Model B as proposed by Gidaspow (1994) where the pressure drop is only in the gas phase and is not shared by the solid phase as is described by Model A. For monosized particles there is little difference between both models (Feng and Yu, (2004a); Kafui et al. (2004)), for the fluidization of binary mixtures Model B is preferred (Feng and Yu, (2004b)). Although in this simulation two particle sizes are used they are separated in monosized layers and even if mixed, Model B is preferred.

$$\frac{\partial \varepsilon \rho}{\partial t} + \nabla \cdot \rho \varepsilon \mathbf{u} = 0 \qquad (9)$$

$$\frac{\partial \varepsilon \rho \mathbf{u}}{\partial t} + \nabla \cdot \rho \varepsilon \mathbf{u} \mathbf{u} =$$
$$\qquad -\nabla p + \nabla \cdot \left(\mu \varepsilon \nabla \mathbf{u} \right) + \rho \varepsilon \mathbf{g} - S \qquad (10)$$

The solid volume fraction is copied from the DEM to the CFD model; the coupling module over-rides the continuity equation for the solid phase such that it is not solved by FLUENT. The momentum coupling causes an additional force on the DEM particles based on the local drag force. In the CFD simulation a momentum sink is added to each of the mesh cells to represent the effect of the momentum transfer to the DEM particles. Consider the momentum sink, P, on a mesh cell:

$$P = \frac{\sum\limits_{DEM\ iterations} \sum\limits_{particles} F}{V} \qquad (11)$$

where F is the force on a particle in a particular iteration from the fluid. The sum is over the number of DEM iterations carried out between CFD iterations which generally have a larger time step than the DEM simulation. The drag force on the individual particles is calculated using the Di Felice (1994) drag model as shown in Equation (12).

$$F_{freestream} = 0.5 C_D \rho_f A_p \left(v_f - v_p \right) \left| v_f - v_p \right|$$
$$F_D = F_{freestream} \varepsilon^{-(\chi+1)}$$
$$C_D = \left(0.63 + \frac{4.8}{\mathrm{Re}^{0.5}} \right)^2 \qquad (12)$$

where ε is voidage and χ is given by:

$$\chi = 3.7 - 0.65 \exp\left[-\frac{\left(1.5 - \log_{10} \mathrm{Re}\right)^2}{2} \right] \qquad (13)$$

MODEL DESCRIPTION

Due to the very high computational demands of DEM modelling it is impossible to model a complete full scale production blast furnace. The geometry used here is based on an experimental blast furnace with a height of app. 7m instead of the approximately 35m of an industrial furnace. Of the 7m of total working height the upper stack is not modelled and only the lower 4m are used. Using experimental blast furnace dimensions allows realistic process modelling with a possibility for validation.

To further reduce the modelling time, the full circumference is not used, rather a cross section over the full width of the furnace. This slot model has parallel, periodic front and back planes through which the particles can exit, reappearing on the opposite side. By using the slot model we effectively lose the 3D cylindrical shape of the blast furnace, however, the geometry is preferred over the alternative pie-slice model. Even though the latter does give a better representation of the 3D cylindrical shape, we are unable to use periodic boundary conditions on the front and back planes resulting in unrealistic particle flow behaviour.

The geometry used is presented in Figure 2, with a height of 4m, a hearth width of 1.2m and a thickness of 6cm. As mentioned before the front and back planes are periodic walls and particles passing trough reappear through the other side. This means the packed bed can be considered more or less infinite at the front and back.

3
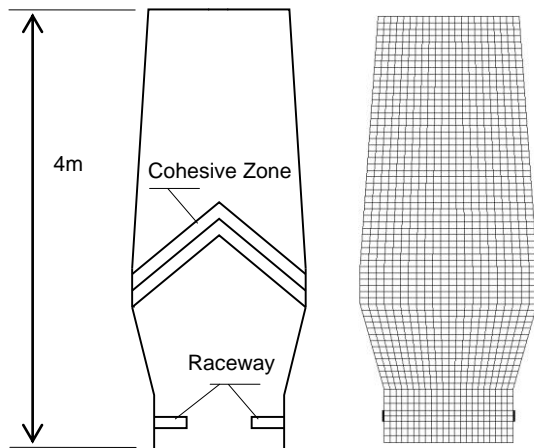
Figure 2: Blast furnace geometry and CFD mesh

At the top the blast furnace is charged with two types of particles: pellets and coke. The latter is non-spherical and is built up from spherical particles, 6 of which surround a central particle. Single spherical particles have a diameter of 1.6cm and the constructed non-spherical particle has a diameter of 3.6cm. Pellets have a diameter of 2cm; both particles are shown below in figure 3. At the start of a simulation the packed bed is filled only with coke on which the first layer of pellets is charged. The coke particles are generated across a large part of the width of the furnace, the pellets in a small area close to the side wall. This creates pellet layers which are becoming thicker close to the wall and correspondingly thickening coke layers in the centre, similar to realistic charging conditions. The furnace contains app. 10500 coke particles consisting of 7 connected particles and 13500 pellets.

Pellet   Coke
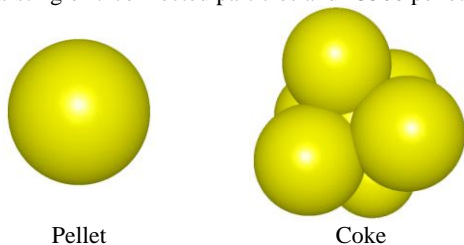
Figure 3: Simulation particles

All particles are removed in geometrically pre-defined regions, the coke particles in the raceway and the pellets in the cohesive zone. To simulate size reduction of the pellets due to melting before total removal, the cohesive zone is defined by three lines. Pellets are reduced in size from 2cm to 1.5cm and 1.5cm to 1cm respectively when passing the upper two lines and are removed when passing the lower. The DEM simulation parameters are shown in table 1.

For CFD simulation the geometry is divided into a grid of 67×22 cells and one cell deep. The cell size is app. 6cm, which gives more averaged values for the bed porosity compared to smaller cells. However, more work is needed to investigate the optimal cell size as well as slot thickness. Gas is injected into the raceways at 20m/s, giving a total flow rate of 0.24 m^3/s, through inlets in the walls indicated by the thick lines in figure 2. Even though the flow rate is higher than in reality, in a real blast furnace the velocity will be considerably higher due the

high temperatures at the raceway. The gas velocity at the top of the furnace is however close to realistic values. Without the inclusion of temperature the model cannot realistically simulate real furnace conditions. The standard k-ε model for turbulence is used. After every 50 DEM time steps, one CFD time step is calculated.

SIMULATION RESULTS AND DISCUSSION

Results from two simulations are presented here: a simulation with only solid particles in Figure 4(b) and one including gas flow in Figure 4(c). The former is a DEM model and the latter is a DEM – CFD coupled model. The CFD results are shown in figure 5. Both simulations are compared at the point where an equal amount of coke has been removed from the furnace, approximately 12400 particles, mainly to compare the solid flow rates. This point requires a longer simulation time when gas flow is included due to the resistance which the descending particle flow encounters from the ascending gas flow. For the simulation including gas flow this is 74.5s compared to 48.9s without. The model at this stage is still under development and future studies will be done to investigate the influence of the simulation parameters, e.g. particle removal rates, cohesive zone shape and location.

	Coke	Pellet
Poisson ratio	0.25	0.25
Shear modulus, *Pa*	1e7	1e7
Density, *kg/m^3*	1000	4000
Coefficient of restitution	0.2	0.2
Coefficient static friction	0.5	0.2
Coefficient rolling friction	0.05	0.02
DEM Time step, *s*	5e-5	

Table 1: DEM Parameters

Layer structure

From the first cross sections shown in Figure 4 the resulting layer structure can be seen. Other than slightly more upward curving layers in the cohesive zone, the case including gas flow has an asymmetrical flow. The layer structure is skewed downwards in the left part of the furnace indicating a higher solid flow velocity. Adding the gas flow to the simulation decreases the stability of the particle flow by loosening the structure and the discrete nature of the model allows the presence of asymmetry It should be remarked here that in the real blast furnace the expansion and contraction of the gas due to the high temperature difference has a significant influence on the materials flow. Including a heat balance in the model is therefore an essential part of this project.

CFD Results

Figure 5 shows some results from the CFD simulation. The solid fraction shows a lower voidage in the pellet bed compared to the coke layers due to the non-spherical shape of the coke particles. This results in higher gas velocities in the pellet layers, as can be seen in the gas velocity figure. High gas velocities can also be seen along the centre line of the furnace due to the larger amount of coke present, the lower porosity has less resistance to gas flow.. The average gas velocity in the packed bed is between 2-4 m/s. Which at the top is close to reality but in the lower furnace is to low due to the isothermal conditions.

No gas flow   *Gas flow*   *No gas flow*   *Gas flow*

DEM Particles: Red – pellets, Grey - coke   Angular velocity *(rad/s)*

Compressive Force *(N)*   Residence time *(s)*
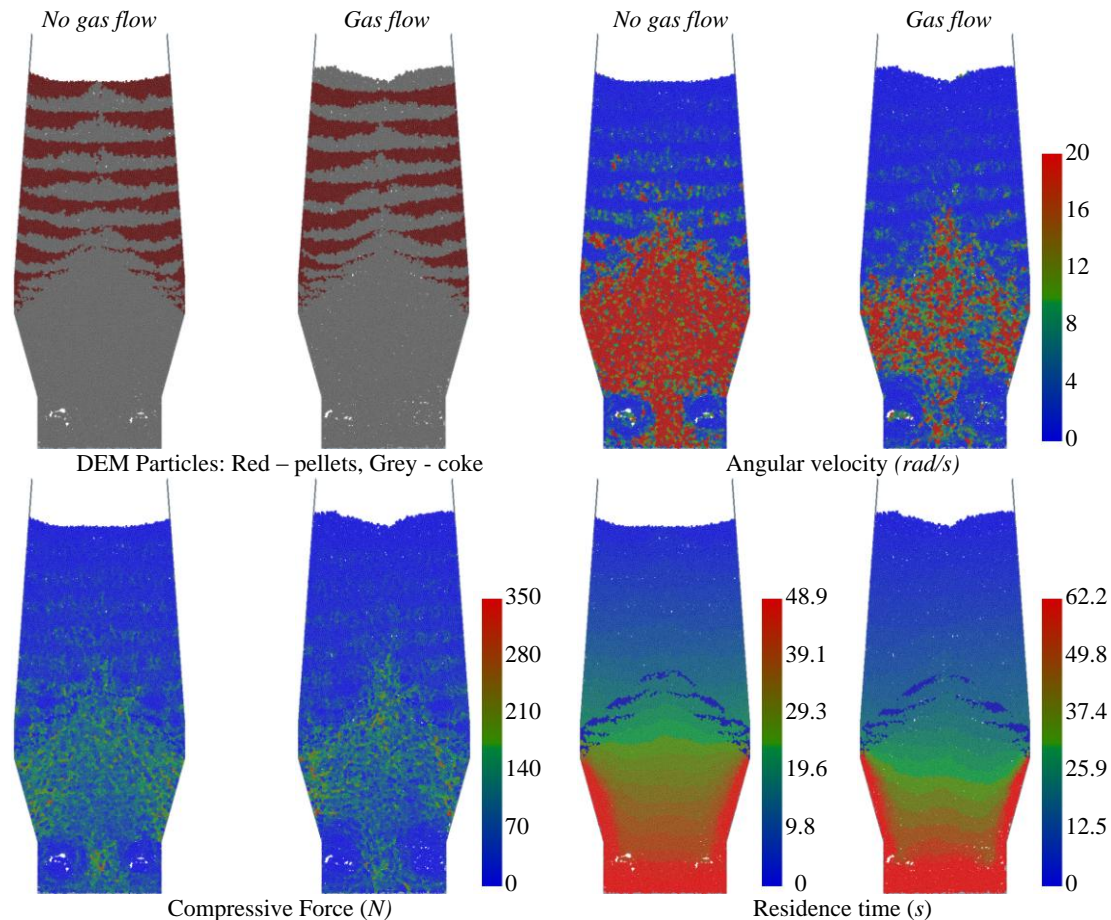
Figure 4: DEM Simulation results

Compressive forces

 The second set of cross sections in Figure 4 shows the compressive forces on the particles creating a dendritic network structure on which the material is resting. In both cases the force network bridges the width of the furnace and is supported by the inward sloping side walls. The network in the simulation without gas flow is considerably larger than in the gas flow case as it is supported by a wider area of the side wall. High velocity injection of gas in the raceway causes the expansion of an area where the particle packing is loose. From Figure 4 can be seen that this area is increased upward when gas flow is included.

Angular velocity

 A clear influence of the gas flow can also be seen from the angular velocity of the particles. In both cases there is very little particle rotation above the cohesive zone due to the widening of the furnace, creating space and thereby reducing shear, and the removal of the particles in the cohesive zone drawing them down across the full width. When the pellets have been removed the non-spherical particles in the remaining coke bed start rotating considerably more. Once in the raceways the rotation is again lower due to its loosened structure. When applying gas flow, the loosening of the structure also causes reduced rotation which can be seen throughout the packed bed. The raceway size increases as the gas velocity increases. . Adding the gas flow should realistically considerably increase the particle rotation in the raceway. However, because on a particle centre only a single

velocity value of the cell surrounding it is working, it does not generate any rotation. Saffman lift is not included in these simulations.

Residence time

Another important flow indicator is the particle residence time. In both figures the colour scale is from red for particles that have been in the simulation since the beginning to blue which are the newest. Below the cohesive zone the separately charged coke layers can be distinguished by their residence times. Two main differences can be seen from the models: there is a much larger particle hold-up along the lower walls in the non-gas model, and there is a more distinct **W**-shape of the coke layers in the lower furnace. The less loosely packed structure of the bed without gas flow increases the particle pressure on the side-walls which causes the larger hold-up. The **W**-shape indicates increased flow above the raceway which, as seen earlier, is much larger and looser in the gas flow case. This causes the more horizontal layer structure in the non-gas case to become **W**-shaped.

CONCLUSION

This paper has presented the first results of an investigation of the influence of gas flow on the solid flow in the ironmaking blast furnace. The work is part of a project to develop a model to predict the cohesive zone by combining DEM particle flow, CFD gas flow and additional models for thermodynamics and kinetics.
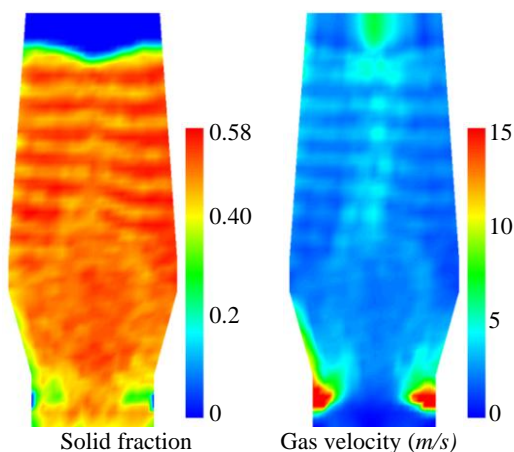
Figure 5: CFD Simulation results

The simulation results show a clear influence of the gas flow mainly on the loosening of the packed bed structure which manifests itself in a more heterogeneous solid flow, a smaller force network and increased particle rotation. Injection of the gas causes an expansion of the raceway area.

Even though the influence of the gas flow can be seen from the previous points, there is no large change in the layer structure itself. It is expected however, that the addition of temperature will have a significant influence on both the material flows.

ACKNOWLEDGEMENTS

REFERENCES

ADEMA, AT., YANG, Y. and BOOM, R., (2008), "DEM Simulation of solid flow in an ironmaking blast furnace – influence of non-spherical particles", *International Symposium, Recent Progress on Mathematical Modelling in Ironmaking.*, Tokyo, Japan, October 16-17.

YAGI, J.-I., (1993), "Mathematical modeling of the flow of four fluids in a packed bed", *ISIJ International*, **33**, 619-639.

AUSTIN, P.R., NOGAMI, H. and YAGI, J.-I., (1997), "A mathematical model of four phase motion and heat transfer in the blast furnace", *ISIJ International*, **37**, 458-467.

DE CASTRO, J.A., NOGAMI, H. and YAGI, J.-I., (2002), "Three-dimensional multiphase mathematical modeling of the blast furnace based on the multifluid model", *ISIJ International*, **42**, 44-52.

NOGAMI, H., CHU, M. and YAGI, J.-I., (2005), "Multi-dimensional transient mathematical simulator of blast furnace process based on multi-fluid and kinetic theories", *Computers and Chemical Engineering*, **29**, 2438-2448.

ZAIMI, S.A., AKIYAMA, T., GUILLOT, J.-B. and YAGI, J.-I., (2000), "Sophisticated multi-phase multi-flow modeling of the blast furnace", *ISIJ International*, **40**, 322-331.

ZAIMI, S.A., SERT, D., GUILLOT, J.-B. and BIAUSSER, H., (2004), "Recent advances in the modelling of solid flows in the blast furnace", *Steel Research International*, **75**, 302-307.

ZHANG, S.J., YU, A.B., ZULLI, P., WRIGHT, B. and AUSTIN, P., (2002), "Numerical simulation of solids flow in a blast furnace", *Applied Mathematical Modelling*, **26**, 141-154.

ZHANG, S.J., YU, A.B., ZULLI, P., WRIGHT, B and TUZUN, U., (1998), "Modelling of the solids flow in a blast furnace" *ISIJ International*, **38**, 1311-1319.

DANLOY, G., MIGNON, J., MUNNIX, R., DAUWELS, G. and BONTE, L., (2001), "A blast furnace model to optimize the burden distribution". *ICSTI Ironmaking Conference*, 37-48.

MATSUZAKI, S., NISHIMURA, T., SHINOTAKE, A., KUNITOMO, K., NAITO, M. and SUGIYAMA, T., (2006), "Development of mathematical model of blast furnace", *Nippon Steel Technical Report*, **94,** 87-95.

ZHOU, Z.Y., ZHU, H.P., YU, A.B., WRIGHT, B. and ZULLI, P., (2008), "Discrete particle simulation of gas-solid flow in a blast furnace", *Computers and Chemical Engineering*, **32**, 1760.

KAWAI, H. and TAKAHASHI, H., (2004), "Solid behavior in shaft and deadman in a cold model of blast furnace with floating-sinking motion of hearth packed bed studied by experimental and numerical DEM analyses" *ISIJ International*, **44**, 1140-1149.

NOUCHI, T., TAKEDA, K. and YU, A.B., (2003) "Solid flow caused by buoyancy force of heavy liquid", *ISIJ International*, **43**, 187-191.

NOUCHI, T., SATO, T., SATO, M., TAKEDA, K. and ARIYAMA, T. (2005), "Stress field and solid flow analysis of coke packed bed in blast furnace based on DEM", *ISIJ International*, **45**, 1426-1431.

MINDLIN, R.D. and DERESIEWICZ, H. (1953), "Elastic spheres in contact under varying oblique forces", *Journal of Applied Mechanics*, **20**, 327-344

ZHU, H.D., ZHOU, Z.Y., YANG, R.Y., YU, A.B. (2007) "Discrete particle simulation of particle systems: Theoretical developments", *Chemical Engineering Science*, **62**, 3378-3396

GIDASPOW, D. (1994), "Multiphase flow and fluidization", Academic press, San Diego

FENG, Y.Q., YU, A.B., (2004a), Comments on "Discrete particle-continuum fluid modelling of gas-solid fluidised beds" by Kafui et al. *Chemical Engineering Science*, **59**, 719-722

KAFUI, K.D., THORNTON, C., ADMAS, M.J., (2004) Reply to comments by Feng and Yu on "Discrete particle-continuum fluid modelling of gas-solid fluidised beds", *Chemical Engineering Science,* **59**, 723-725

FENG, Y.Q., YU, A.B., (2004b) "Assessment of model formulations in the discrete particle simulation of gas-solid flow", *Industrial and Engineering Chemistry Research*, **43**, 8378-8390

DIFELICE, R. (1994), "The voidage function for fluid-particle interaction systems", *International Journal of Multiphase Flow*, **20**, 1, 153-159